Crystallographic texture engineering through novel melt strategies via electron beam melting: Inconel 718

R. R. Dehoff*[1,2], M. M. Kirka[1,2], F. A. List III[1,2], K. A. Unocic[2] and W. J. Sames[1,3]

Preliminary research has demonstrated the ability to utilise novel scan strategies in the electron beam melting (EBM) process to establish control of crystallographic texture within Inconel 718 deposits. Conventional EBM scan strategies and process parameters yield coarse columnar grains aligned parallel to the build direction. Through varying process parameters such as beam power, beam velocity, beam focus and scan strategy, the behaviour of the electron beam can be manipulated from a line source to a point source. The net effect of these variations is that the resulting crystallographic texture is controlled in a manner to produce either epitaxial deposits or fully equiaxed deposits. This research demonstrates the ability to change the crystallographic texture on the macroscale indicating that EBM technology can be used to create complex geometric components with both site-specific microstructures and material properties.

Keywords: Additive manufacturing, Electron beam melting, Texture, Nickel-base superalloy

This paper is part of a special issue on Additive manufacturing

Introduction

The term additive manufacturing (AM) encompasses a broad range of technologies with the capability to make complex three-dimensional structures from feedstock material. Typically material is added layer by layer or point by point in order to build up metal, polymer, ceramic, or composite structures. Metal processes using a melt pool (similar to welding) are divided into two main categories; directed energy deposition and powder bed fusion. Typically, powder based additive manufacturing technologies such as electron beam melting (EBM) have been utilised to make highly intricate components while directed energy systems have been focused in repair of existing components and production of near net shapes.

To date much of the focus in developing AM processes has been towards producing fully dense and delamination free deposits which as a byproduct result produce epitaxial deposits with the texture oriented parallel to the build direction.[1–3] The thought being that epitaxial deposits would be ideal for maximising the mechanical properties of AM built parts as occurs in directionally solidified and single crystal Nickel-base (Ni-base) superalloys loaded along the direction of solidification.[4] However, epitaxial growth does not necessarily correlate to enhanced mechanical performance in all situations, e.g. complex stress states. While not identical, the cooling rates observed in welding and AM processes are similar enough, such that the basic understanding of texture evolution derived from welding processes can be extrapolated to AM process to aid in the development of scan strategies aimed at controlling evolution of the texture at a given point.

As in welding, the important solidification parameters that indirectly require control are growth rate (R), temperature gradient (G), and undercooling (ΔT).[5] Based upon these parameters any of the principle crystallographic planes become possible growth directions for the solidification front; in the case of face centred cubic materials these are the $\langle 001 \rangle$ directions.[6] In epitaxial solidification, the optimum growth direction is the one aligned normal to the thermal gradient between the solid and liquid.[6] Additionally, grains that deviate from that of epitaxial growth have been shown to form under high beam velocity conditions.[6–8] Furthermore, the probability for the nucleation of equiaxed grains ahead of the epitaxial solidification front is increased in the presence of high thermal gradients.[9–11] This change in solidification structure is termed a columnar to equiaxed transition.

While much has been considered on the optimisation of the AM process, the true power of the AM process is being significantly overlooked. Through the AM process, texture has the potential to be controlled at will to produce functionally graded textures throughout an AM part that, in theory, could perform better under complex mechanical loadings than either a single crystal or polycrystalline material would alone. With crystallographic texture control combined with integrated computational materials engineering concepts, the potential

[1]Manufacturing Demonstration Facility, Oak Ridge National Laboratory, Knoxville, TN, USA
[2]Materials Science and Technology Division, Oak Ridge National Laboratory, Oak Ridge, TN, USA
[3]Department of Nuclear Engineering, Texas A&M University, College Station, TX, USA

*Corresponding author, email dehoffrr@ornl.gov

Published by Maney on behalf of the Institute
Received 30 June 2014; accepted 15 October 2014
DOI 10.1179/1743284714Y.0000000697

for a new era of engineering design is possible. Within this work is presented a preliminary demonstration of microstructure control through variations in the scan strategy of an electron beam AM process on the γ'' strengthened Ni-base superalloy Inconel 718 that has a primary use in high temperature applications.

Experimental procedures and methods

Samples were fabricated using rotary atomised powder of the Ni-base superalloy Inconel 718; the chemistry is discussed elsewhere.[12] The size distribution of the powder particles was in the mesh size range of $-100+325$. For the EBM process an Arcam A2 electron beam system was utilised. A control sample was fabricated using standard Inconel 718 deposition parameters developed by Arcam of geometry described elsewhere.[13] To examine the influence of beam scan strategy, eight specimens were arranged across the diagonal of a 150×150 mm build plate as shown in Fig. 1, with the build direction being along the Z-direction. All of the specimens had dimensions of $10\times10\times10$ mm. Each of the samples were fabricated using proprietary beam scan strategies that included variations to the beam path, beam speed, and melting current that allow for a transition between line source and point source beam conditions. During melting, the beam current was maintained within a range of 4–6 mA for each of the scan strategies. Furthermore, layer thicknesses of 50 μm were used.

Microstructural analysis was conducted on specimens labelled A, B and C; these represent the extremes of the scan strategies tested. To characterise the influence of the scan strategies on the resultant microstructures, the specimens were sectioned along the faces parallel (XZ plane) and perpendicular (XY plane) to the build direction and polished successively using SiC abrasive paper ending with a final 0·04 μm colloidal silica polish. The polished specimens were then analysed using a JEOL 6500 field emission gun scanning electron microscope equipped with an EDAX electron backscatter diffraction detector (EBSD). Further characterisation of the resultant specimen texture was undertaken with X-ray diffraction (XRD) analysis.

Results and discussion

Much of the thought in EBM and AM process development has been towards the optimisation of process parameters (beam current and beam velocity) such that fully dense and geometrically accurate parts are achievable with minimal concern for the resulting microstructure. Figure 2 shows the typical Inconel 718 macrostructure obtained from utilising standard Arcam build parameters. Overall the microstructure exhibits a high degree of texture, with the [001] crystallographic orientation aligned parallel to the build direction as indicated by the EBSD map in Fig. 2*b*, where the red colour corresponds to the [001] crystallographic grain orientation in the inverse pole figure for nickel. Furthermore, the EBSD pole figures (Fig. 2*c*) affirm that the grain structure is a highly oriented columnar structure, i.e. the structure is directionally solidified. As discussed previously, this result is highly typical within AM processes.[13]

For some time, it has been well known that through controlling the temperature gradient and velocity of the

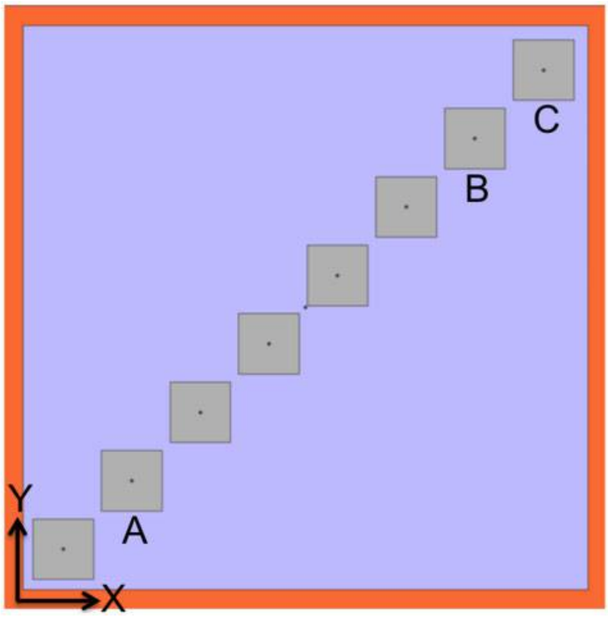

1 Build layout on 150×150 mm Arcam plate with specimens associated with Scan Strategies A, B and C denoted by A, B and C respectively

liquid/solid interface, the solidification microstructure can transition from columnar to equiaxed.[9,14,15] The net impetus for this transition being that a constitutionally undercooled zone forms ahead of the solidification front that causes spontaneous nucleation of grains.[9] While the thermal gradients in the EBM process are multi-dimensional, the Inconel 718 solidification map (Fig. 3) for an one-dimensional temperature gradient with the Arcam process window indicated by the dashed box.[13] While modelling the solidification process is computationally intensive, the basic principles of the columnar to equiaxed transition can be applied within the scan strategies used.

Deviations from the standard Arcam process parameters pose challenges such as the generation of unwanted porosity, layer delamination, and differences in thermal exposure throughout the build process. The ability to maintain texture control throughout a desired region is an additional challenge as a result of the above in addition to the ability to form stray grains. Recent work has shown the hold temperature and hold time of an EBM build to be an influencing factor on the size, shape, and distribution of precipitates within the deposits and to be of minimal influence on the crystallographic texture of the deposits.[13] A subset of the scan strategies attempted is presented below to showcase the results that ultimately produced three unique textures that differed from the standard texture throughout the entirety of the specimen with exception to the build plate interface region. These strategies are referred to as Scan Strategy A, B, and C, with their location in the build labelled in Fig. 1.

Similar to the texture observed in the standard scan strategy (Fig. 2), Scan Strategy A resulted in an epitaxial deposit as evidenced by the EBSD results for the XY plane (Fig. 4). Generally, the presence of coarser grains within the deposit can be attributed to the relatively slower cooling rate when compared to the ones observed when melting with the standard parameters. Furthermore,

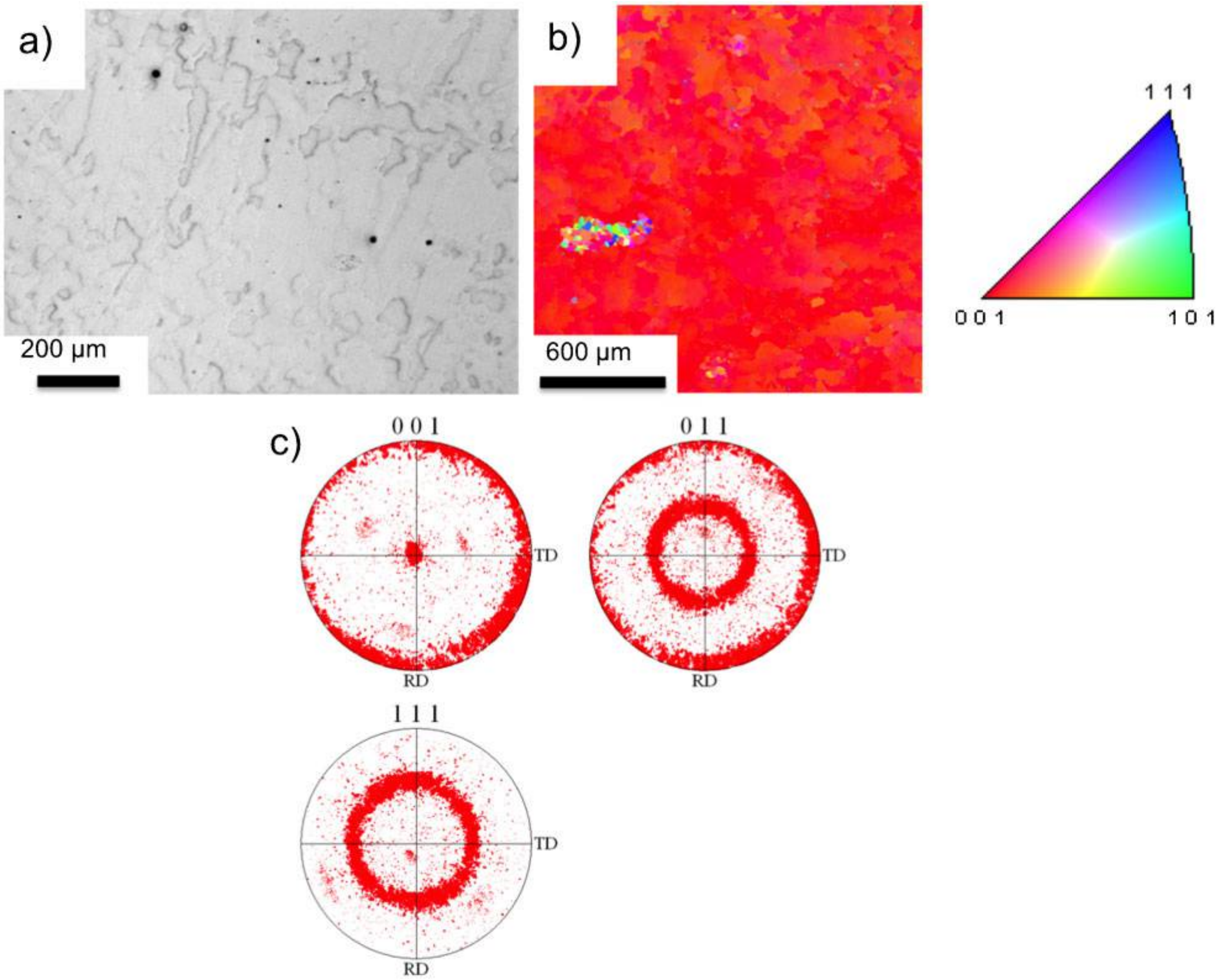

a SEM micrograph; *b* EBSD orientation map; *c* EBSD pole figures for (001), (011) and (111) planes
2 Inconel 718 texture obtained through standard Arcam process parameters for XY plane

the deposit can be considered single crystal quality within the $\pm 7{\cdot}5^{\circ}$ industry standard due to the high concentration of grains at the centre of the (200) pole figure (Fig. 4) and

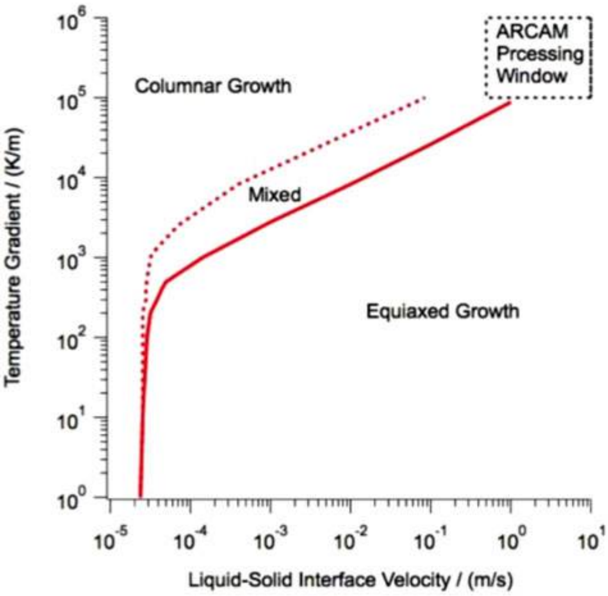

3 Solidification map for Inconel 718 depicting columnar to equiaxed transition and Arcam EBM processing window

the pair of concentrations in the ⟨110⟩ directions in the (111) pole figure (Fig. 4).[16]

The results of Scan Strategy B are given in Fig. 5 for both the XY plane and XZ plane. The EBSD results indicate that although large columnar-like grains are present, they exhibit stochastic orientations similar to an equiaxed structure. X-ray diffraction analysis shown in Fig. 5*c* and *d* further confirms this decrease in texture through randomness of the grain distribution in both the (200) and (111) pole figures (Fig. 5). Ultimately the presence of the equiaxed grain structure gives indication that Scan Strategy B is able to produce a combination of G and R within the melt pool such that the solidification conditions are fully within the equiaxed zone of the Arcam process window (Fig. 3). In addition, turbulent fluid flow and spurious grain growth within the melt pool can also be considered as attributable for the equiaxed grain state.[9,11] Within the build direction (Fig. 5) the grains exhibit lengths within the range of one to two layer thicknesses. This can be considered the result of the partial remelting of the previous deposited layer combined with the lower free energy barrier promoting the continued growth of underlying grains until terminated by other grains.[17]

Unlike the typical textures that arose from Scan Strategies A and B, Scan Strategy C resulted in the grain texture oriented transverse to the build direction as

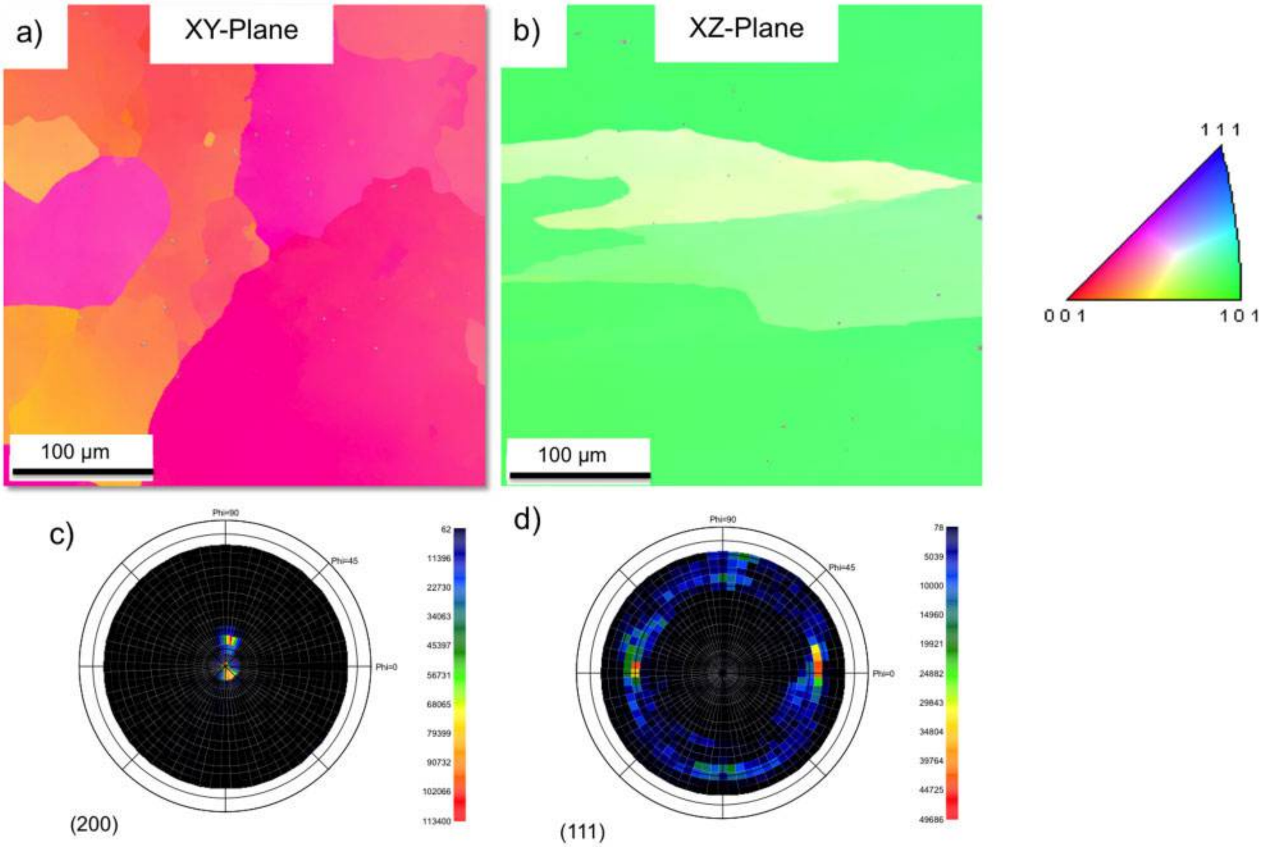

4 Resultant texture of Scan Strategy A: *a* EBSD of XY-plane, *b* EBSD of XZ plane; *c* (200) XY plane XRD pole figure and *d* (111) XY plane XRD pole figure

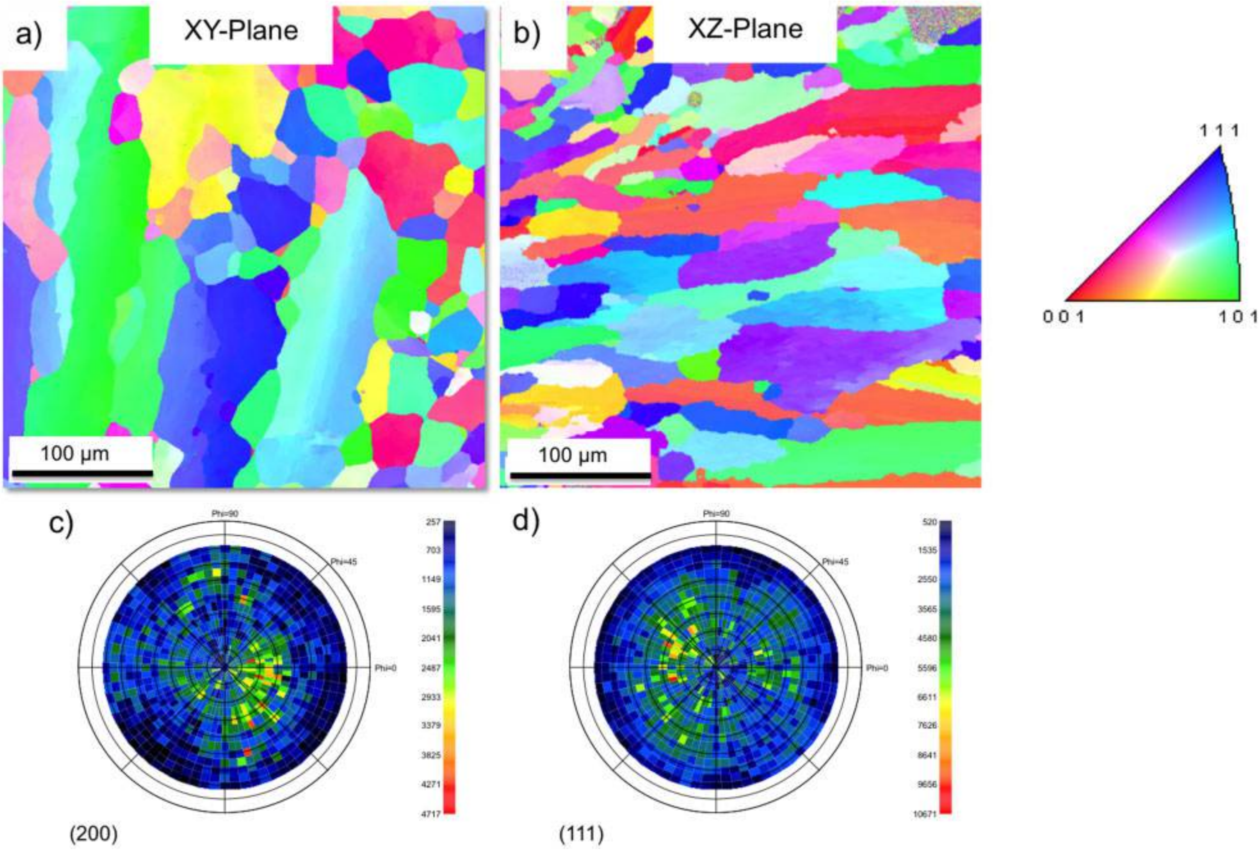

5 Resultant texture of Scan Strategy B: *a* EBSD of XY plane; *b* EBSD of XZ plane; *c* (200) XY plane XRD pole figure and *d* (111) XY plane XRD pole figure

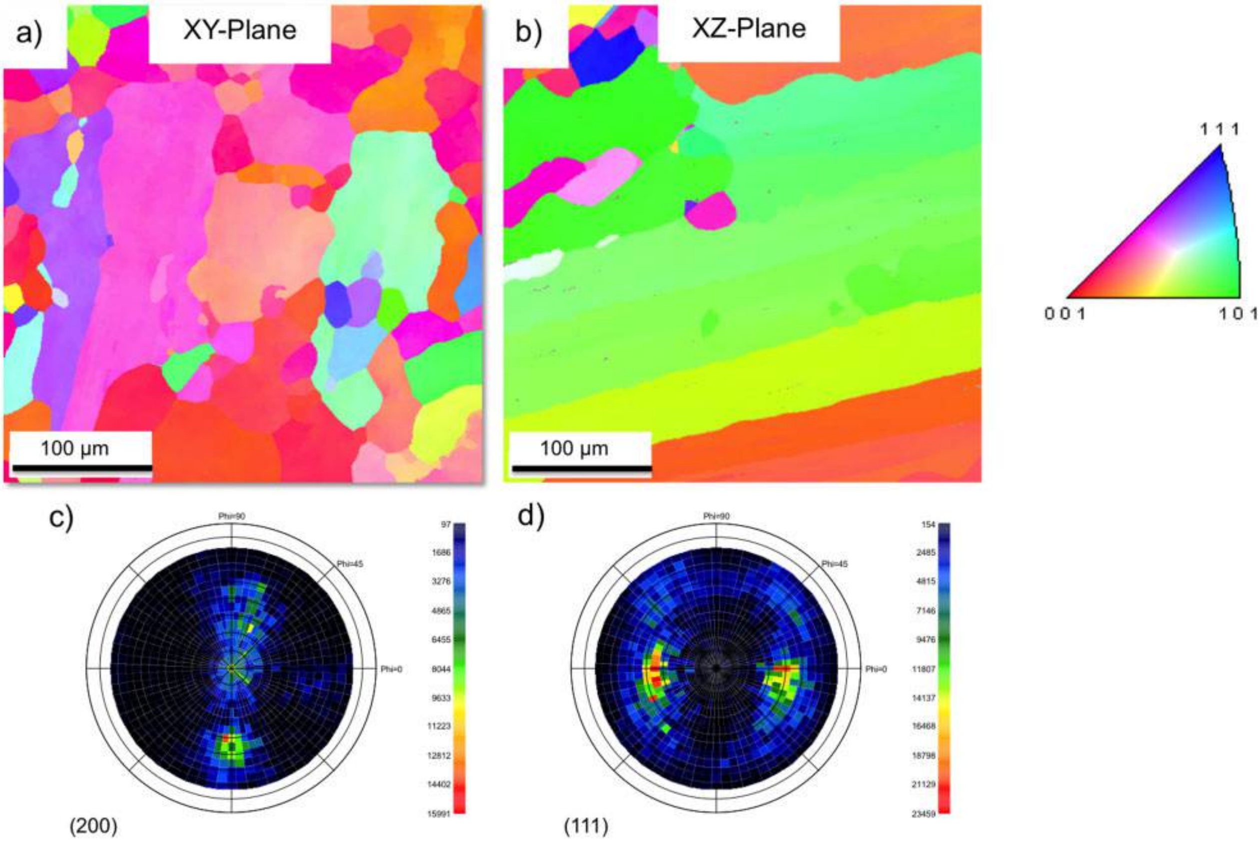

6 Resultant texture of Scan Strategy C: *a* EBSD of XY plane; *b* EBSD of XZ plane; *c* (200) XY plane XRD pole figure and *d* (111) XY plane XRD pole figure

shown in Fig. 6. This is particularly evident in the grain orientation density band that passes vertically across the (200) pole figure. Within the welding literature similar experimental observations have been found, where this occurrence is attributable to the solidification front moving at the same speed as the electron beam.[5] However, the interesting aspect of these results is that the entire structure is composed of grains that are all nearly aligned with their [001] crystallographic direction transverse to the build direction.

Conclusions

By varying the parameters and scan strategy of the electron beam from a line source to a point source, solidification conditions that give rise to both columnar and equiaxed conditions were determined. Specifically, through these variations in the scan strategy, the texture was shown capable of having the [001] aligned parallel to the build direction, the [001] transverse to the build direction, and random texture as affirmed by XRD analysis. In the case of the equiaxed grain structure, the grain thickness was found to be approximate to one to two layer thicknesses used in the build. Ultimately, the results presented here indicate that through control of the process parameters, texture can be controlled. Additional studies are currently underway in order to understand the minimum length scale of grain formation as well as the maximum control possible on grain orientation.

Acknowledgements

Research sponsored by the US Department of Energy, Office of Energy Efficiency and Renewable Energy, Advanced Manufacturing Office, under contract DE-AC05-00OR22725 with UT- Battelle, LLC. Additionally this research was supported by fellowship funding provided by the US Department of Energy, Office of Nuclear Energy, Nuclear Energy University Programs. The United States Government retains and the publisher, by accepting the article for publication, acknowledges that the United States that the United States Government retains a non-exclusive, paid-up, irrevocable, world-wide license to publish or reproduce the published form of this manuscript, or allow others to do so, for United States Government purposes.

References

1. L. Murr, E. Martinez, S. Gaytan, D. Ramirez, B. Machado, P. Shindo, J. Martinez, F. Medina, J. Wooten, D. Ciscel, U. Ackelid and R. Wicker: 'Microstructural architecture, microstructures, and mechanical properties for a nickel-base superalloy fabricated by electron beam melting', *Met. Mater. Trans. A*, 2011, **42A**, 3491–3508.
2. D. A. Ramirez, L. E. Murr, E. Martinez, D. H. Hernandez, J. L. Martinez, B. I. Machado, F. Medina, P. Frigola and R. B. Wicker: 'Novel precipitate–microstructural architecture developed in the fabrication of solid copper components by additive manufacturing using electron beam melting', *Acta Mater.*, 2011, **59**, 4088–4099.
3. N. Hrabe, R. Kircher and T. Quinn: 'Effects of processing on microstructure and mechanical properties of Ti–6Al–4V fabricated using electron beam melting (EBM): Orientation and location', Proc. 15th Solid Freeform Fabrication Symp., Austin, TX, USA, August 2004, Laboratory for Freeform Fabrication, 1045–1058.
4. M. McLean: 'Directionally solidified materials for high temperature service', 1st edn; 1983, London, The Metals Society.
5. S. A. David and J. M. Vitek: 'Correlation between solidification parameters and weld microstructures', *Int. Mater. Rev.*, 1989, **34**, 213–245.
6. M. Rappaz, S. A. David, J. M. Vitek and L. A. Boatner: 'Development of microstructures in Fe15Ni15Cr single crystal

electron beam welds', *Met. Mater. Trans. A*, 1989, **20A**, 1125–1138.
7. J. M. Vitek: 'The effect of welding conditions on stray grain formation in single crystal welds–theoretical analysis', *Acta Mater*., 2005, **53**, 53–67.
8. S. S. Babu, S. A. David, J. W. Park and J. M. Vitek: 'Joining of nickel base superalloy single crystals', *Sci. Technol. Weld. Join*., 2004, **9**, 1–12.
9. M. Gäumann, C. Bezençon, P. Canalis and W. Kurz: 'Single-crystal laser deposition of superalloys: processing–microstructure maps', *Acta Mater.*, 2001, **49**, 1051–1062.
10. M. Gäumann, S. Henry, F. Cleton, J. D. Wagniere and W. Kurz: 'Epitaxial laser metal Forming: analysis of microstructure formation', *Mater. Sci. Eng. A*, 1999, **A271**, 232–241.
11. S. Mokadem, C. Bezençon, A. Hauert, A. Jacot and W. Kurz: 'Laser repair of superalloy single crystals with varying substrate orientations', *Met. Mater. Trans. A*, 2007, **38A**, 1500–1510.
12. K. A. Unocic, L. M. Kolbus, R. R. Dehoff, S. N. Dryepondt and B. A. Pint: 'High-temperature performance of UNS N07718 processed by additive manufacturing', Corrosion 2014, San Antonio, TX, USA, March 2014, NACE International.
13. W. Sames, K. Unocic, R. Dehoff, T. Lolla and S. Babu: 'Thermal effects on microstructural heterogeneity of Inconel 718 materials fabricated by electron beam melting', *J. Mater. Res*., 2014, 10.1557/jmr.2014.140.
14. J. Beuth and N. Klingbeil: 'The role of process variables in laser-based direct metal solid freeform fabrication', *JOM*, 2004, **53**, 36–39.
15. J. D. Hunt: 'Steady state columnar and equiaxed growth of dendrites and eutectic', *Mater. Sci. Eng*., 1984, **65**, 75–83.
16. R. Reed: 'The superalloys fundamentals and applications', 1st edn; 2006, London, Cambridge University Press.
17. W. Kurz and D. J. Fisher: 'Fundamentals of solidification', 3rd edn; 1992, London, Trans Tech Publications.